Fine Epitope Mapping of Monoclonal Antibody 5F1 Reveals Anticatalytic Activity toward the N Domain of Human Angiotensin-Converting Enzyme†

Sergei M. Danilov,*,‡ Jean M. Watermeyer,§ Irina V. Balyasnikova,‡ Kerry Gordon,§ Elena V. Kugaevskaya,|| Yulia E. Elisseeva,|| Ronald F. Albrecht, II,‡ and Edward D. Sturrock§

Department of Anesthesiology, University of Illinois at Chicago, Chicago, Illinois 60612, Division of Medical Biochemistry, Institute of Infectious Diseases and Molecular Medicine, University of Cape Town, Observatory 7925, South Africa, and Institute of Biomedical Chemistry, Moscow, Russia

Received March 11, 2007; Revised Manuscript Received April 27, 2007

ABSTRACT: Angiotensin I-converting enzyme (ACE, peptidyl dipeptidase, EC 3.4.15.2) is a key enzyme in cardiovascular pathophysiology. A wide spectrum of monoclonal antibodies to different epitopes on the N and C domains of human ACE has been used to study different aspects of ACE biology. In this study we characterized the monoclonal antibody (mAb) 5F1, developed against the N domain of human ACE, which recognizes both the catalytically active and the denatured forms of ACE. The epitope for mAb 5F1 was defined using species cross-reactivity, synthetic peptide (PepScan technology) and phage display library screening, Western blotting, site-directed mutagenesis, and protein modeling. The epitope for mAb 5F1 shows no overlap with the epitopes of seven other mAbs to the N domain described previously and is localized on the other side of the N domain globule. The binding of mAb 5F1 to ACE is carbohydrate-dependent and increased significantly as a result of altered glycosylation after treatment with α-glucosidase-1 inhibitor, *N*-butyldeoxynojirimycin (NB-DNJ), or neuraminidase. Out of 17 species tested, mAb 5F1 showed strict primate ACE specificity. In addition, mAb 5F1 recognized human ACE in Western blots and on paraffin-embedded sections. The sequential part of the epitope for mAb 5F1 is created by the N-terminal part of the N domain, between residues 1 and 141. A conformational region of the epitope was also identified, including the residues around the glycan attached to Asn117, which explains the sensitivity to changes in glycosylation state, and another stretch localized around the motif ^{454}TPPSRYN^{460}. Site-directed mutagensis and inhibition assays revealed that mAb 5F1 inhibits ACE activity at high concentrations due to binding of residues on both sides of the active site cleft, thus supporting a hinge-bending mechanism for substrate binding of ACE.

Angiotensin I-converting enzyme (ACE)[1] (EC 3.4.15.1, CD 143) is a zinc metallopeptidase responsible for the formation of the vasoconstrictor angiotensin II and the inactivation of the vasodilator bradykinin. The enzyme is also involved in neuropeptide metabolism and reproductive and immune functions (for reviews see refs *1*−*4*). The somatic isoform is expressed widely at surface−fluid interfaces and plays an important role in blood pressure regulation, the development of vascular pathology, and endothelium remodeling in some disease states. High ACE expression is a characteristic of endothelial (*5*) and dendritic cells (*6*) as well as of endothelial progenitor cells (EPC) (Danilov et al., unpublished observations). Furthermore, ACE has been assigned as a CD marker, CD 143 (*7*, *8*).

Somatic ACE consists of two homologous domains (N and C domains), each having a functional active site (*9*). A testis-specific isoform, consisting of the C domain of somatic ACE with an additional 36-residue O-glycosylated region at its N-terminus, is transcribed from a tissue-specific promoter in intron 12 of the ACE gene (*10*). The tertiary structure of somatic ACE is still unknown; however, the crystal structures of the N domain of human ACE and of human testis ACE (equivalent to the C domain) were recently described (*11*, *12*). Moreover, some ideas about the arrangement of the N and C domains in somatic ACE have been proposed (*12*, *13*).

Development of numerous mAbs to different epitopes of ACE which influence ACE function, in conjunction with epitope mapping, provides a unique opportunity to study the structural basis for a variety of important biological processes. For example, the study of the effect of mAbs on ACE shedding (*14*) or ACE dimerization in reverse micelles (*15*) in conjunction with the epitope mapping of functionally active antibodies allowed us to identify the region on the N domain that is likely to be responsible for the low rate of somatic ACE shedding and ACE dimerization (*16*). One of

† This work was supported in part by the University of Cape Town and the South African National Research Foundation.

* Corresponding author. Phone: (312) 413-7526. Fax: (312) 996-9680. E-mail: danilov@uic.edu.

‡ University of Illinois at Chicago.

§ University of Cape Town.

|| Institute of Biomedical Chemistry.

[1] Abbreviations: ACE, angiotensin-converting enzyme; Hip-His-Leu, hippuryl-L-histidyl-L-leucine; Z-Phe-His-Leu, benzyloxycarbonylphenylalanyl-L-histidyl-L-leucine; CHO, Chinese hamster ovary; mAb, monoclonal antibody; ELISA, enzyme-linked immunosorbent assay; CD markers, cluster designation markers; PBS, phosphate-buffered saline; CHAPS, 3-[(3-cholamidopropyl)dimethylammonio]-1-propanosulfonate; TMB, tetramethylbenzidine; NB-DNJ, *N*-butyldeoxynojirimycin.

10.1021/bi700489v CCC: $37.00
Published on Web 07/14/2007

the mAbs, 3A5, which greatly influences ACE shedding (*14*), also demonstrated strong anticatalytic activity (*17*, *18*). Localization of the epitope for another monoclonal antibody, 1B3, allowed the development of a new, sensitive method for the detection of an ACE mutation using plasma samples (*19*). Recently, we defined the epitopes for two other mAbs to the N domain of ACE, 1G12 and 6A12, and developed a highly sensitive method for the detection and quantification of ACE inhibitors in human blood (*13*).

There are a number of reasons why it is important to determine the fine epitope mapping of these mAbs. First, interpretation of immunofluorescence data requires the use of mAbs that recognize distinct epitopes on the molecule of interest. Second, the complexity of the posttranslational processing of ACE (*5*, *6*) makes it desirable to define exactly which intermediates will be recognized by which antibodies. Third, site-specific antibodies are potentially valuable reagents to study the role of structural domains of ACE. Finally, the presence of anti-ACE autoantibodies was indicated recently in several diseases with an autoimmune component, such as lupus erythrematosis, scleroderma, and rheumatoid arthritis (*14*, *20*; Danilov, Matucci-Cerinic, et al., unpublished observations). The clinical significance of the presence of these autoantibodies is still unclear; however, it is possible that the epitope specificity of the ACE autoantibodies for these distinct diseases could be characteristic of the pathology. Therefore, fine epitope mapping of these monoclonal ACE antibodies might help to elucidate the molecular mechanisms involved in the development of autoantibodies to ACE in different diseases.

In this study we define the epitope for mAb 5F1, a mAb that recognizes both catalytically active and denatured human ACE, and gain important insight into the dynamics of the molecule during substrate and inhibitor binding.

MATERIALS AND METHODS

Chemicals. Benzyloxycarbonyl-L-phenylalanyl-L-histidyl-L-leucine (Z-Phe-His-Leu) was obtained from Bachem (King of Prussia, PA). Hippuryl-L-histidyl-L-leucine (Hip-His-Leu) and other reagents (unless otherwise indicated) were obtained from Sigma (St. Louis, MO).

Expression of Human ACE Constructs in CHO Cells. Constructs tACEΔ36 (human testis ACE lacking the N-terminal O-glycosylated 36 residues) (*21*), D629 (residues 1−629 of somatic ACE, comprising the N domain and 17 residues of the interdomain linker) (*22*), Nfr737 (residues 1−737 of somatic ACE, comprising the N domain and linker with an additional 108 residues from the C domain) (*23*), and chimeric ACE mutants (human tACEΔ36 substituted with regions of the N domain sequence) (*24*) were generated previously. Chimera C1-141Ndom (previously NdelACE) has tACEΔ36 residues 37−163 replaced with homologous N domain residues 1−141, C395-557Ndom has tACEΔ36 residues 417−579 replaced with N domain residues 395−557, and C561-601Ndom has tACEΔ36 residues 583−623 replaced with N domain residues 561−601. Stable cell lines of CHO cells expressing wild-type human somatic ACE (clone 2C2), tACEΔ36, D629, Nfr737, and the ACE chimeras were cultured as described previously (*21*−*25*). CHO-ACE cells at confluence were washed gently with PBS and incubated for 24−48 h with serum-free Ultra-CHO medium (Cambrex Bioscience Walkersville, Inc., Walkersville, MD) or OPTI-MEM (Invitrogen Corp.) without FBS. Culture medium was collected as a source of soluble ACE, whereas cell lysate was prepared with 8 mM CHAPS as a source of the membrane-bound form of ACE (*14*, *25*). In the experiments with restricted glycosylation, the cells were grown using serum-free Ultra-CHO medium containing 2 mM *N*-butyldeoxynojirimycin (NB-DNJ), an inhibitor of the oligosaccharide-processing enzymes α-glucosidases I and II. This medium was changed twice over a period of 5 days before harvesting. For Western blotting, tACEΔ36, D629, and the chimeric ACE mutants were purified by lisinopril affinity chromatography as described previously (*26*).

Antibodies. The properties of a set of monoclonal antibodies directed to different epitopes located on the N domain of ACE are described in detail elsewhere (*13*−*19*).

ACE activity was assayed fluorometrically with different substrates, Hip-His-Leu and Z-Phe-His-Leu, as described (*27*, *28*). For the inhibition assay, the N domain of ACE (D629; 10 milliunits/mL, determined using Z-Phe-His-Leu) was incubated for 1 h at 37 °C with increasing concentrations (0.01, 0.1, 1.0, and 10 μg/mL) of purified mAb 5F1 or control mAbs before the residual ACE activity was determined with Hip-His-Leu or Z-Phe-His-Leu.

Quantification of ACE Binding by Anti-ACE mAbs. (A) Plate Precipitation Assay. Microtiter plates bound with goat anti-mouse IgG were coated with different anti-ACE mAbs and were incubated with serum-free culture medium or lysates obtained from CHO-ACE cells (wild type or mutants) as a source of soluble or membrane-bound recombinant ACE (*17*). Plasma or serum from human or animal species as well as the supernatant of the homogenates [1:10 (w/v) in 50 mM Tris-HCl and 150 mM NaCl, pH 7.5, with 0.5% Triton X-100] of kidney or lung from the same species was also used as a source of ACE. In some experiments mAbs were adsorbed to the wells of microtiter plates directly, without the goat anti-mouse bridge (*17*, *29*). For inhibition studies, the incubation of ACEs with immobilized mAbs was performed in the presence of lisinopril or EDTA. To investigate the effect of glycosylation, purified preparations of human tissue (seminal fluid) or blood ACE were treated with neuraminidase (Sigma, St. Louis, MO), 0.25 milliunits/mL for 1 h at 37 °C.

The amount of ACE precipitated by a given mAb reflects the binding affinity and was quantified by two methods:

(i) Precipitated ACE activity in the wells was estimated using the substrates Hip-His-Leu or Z-Phe-His-Leu, as described previously (*17*).

(ii) The amount of precipitated ACE protein was quantified by incubation with sheep anti-ACE polyclonal antibodies conjugated with horseradish peroxidase from an ACE ELISA kit (Chemicon Int., Temecula, CA), followed by a spectrophotometric assay with tetramethylbenzidine (TMB) as substrate (*29*).

(B) ELISA. The 96-well microtiter plates (Corning Corp., Corning, NY) were coated with 50 μL of purified human ACE isolated from kidney, lung, or seminal fluid in native or denatured forms (1−5 μg/mL) and incubated overnight at 4 °C. After washing, 50 μL of hybridoma supernatants containing mAbs to ACE or pure mAbs (10 μg/mL) was added and incubated for 2 h at room temperature. The ACE−mAb complex was then incubated with goat anti-

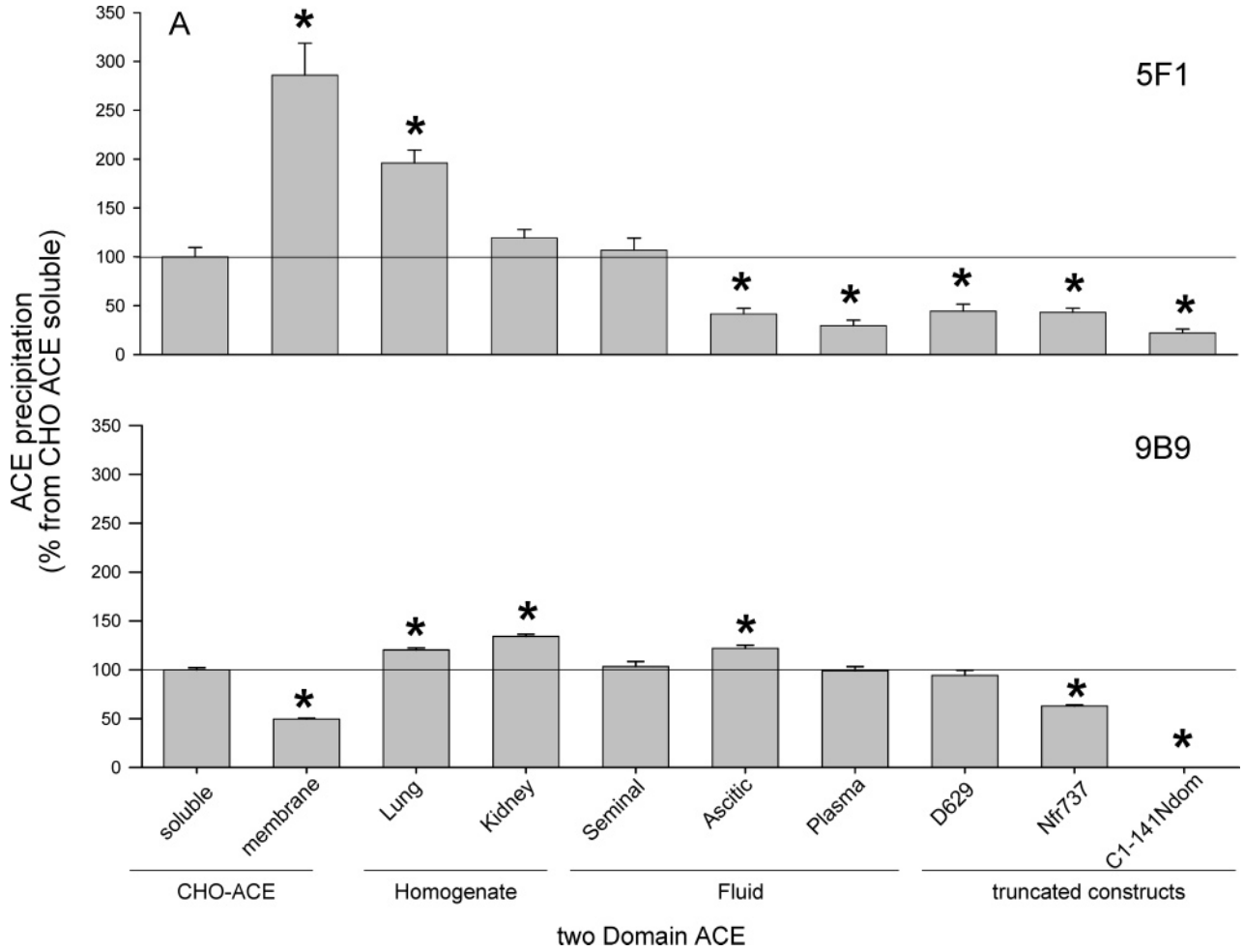

FIGURE 1: Precipitation of different human ACEs by mAb 5F1. Plate precipitation assay. ACE activity in different ACE preparations, human recombinant ACE expressed in CHO cells (membrane-bound and soluble), lung and kidney ACE, soluble ACE from seminal and ascitic fluid and plasma, truncated N-fragments of different lengths (629 and 737 amino acid residues), and ACE chimera C1-141Ndom, was adjusted to a final enzymatic activity of 5−10 milliunits/mL using Z-Phe-His-Leu as a substrate. ACE preparations were then incubated with microtiter plates coated with mAb 5F1 and 9B9 (as a positive control) via goat anti-mouse IgG (*17*). Precipitated ACE activity was quantified spectrofluorometrically using Z-Phe-His-Leu as a substrate. Data were presented as a ratio of precipitation of different ACEs to that of soluble recombinant ACE, expressed in CHO cells.

mouse polyclonal antibody conjugated with alkaline phosphatase (Sigma, St. Louis, MO) diluted 1:1000 with PBS/BSA for 1 h at room temperature and washed afterward. Alkaline phosphatase was developed using *p*-nitrophenyl phosphate as a substrate, and absorbance was read at 405 nm.

The binding of mAb 5F1 to selected peptides was evaluated using a competition ELISA. Microtiter wells were coated with purified human kidney ACE and subsequently blocked with a solution of 0.2% casein; peptide competitors were then added to each well at concentrations of 0.25 and 1 mg/mL, followed immediately by addition of anti-ACE mAb. Hexapeptides ^{451}SGRTPP, ^{457}SRYNFD, ^{535}TKAGAL, and ^{1260}RSLHRH, comprising a selection of sequences of ACE, were synthesized by Biosynthesis, Inc. (Lewisville, TX) and used in competitive ELISA.

Synthetic Peptide Library Screening: PepScan Technology. A series of hexapeptides covering amino acid positions 201−557 [mature somatic ACE numbering (*9*)] in the N domain of human ACE were synthesized on polyethylene pins derivatized with B-alanine residues attached to their surface and arranged in 96-well format (*30*). The interactions of pin-attached hexapeptides with mAb 5F1 were detected by ELISA as described in ref *30*. Nonimmune mouse IgG was used as a negative control.

Phage Display Library Screening. Two filamentous phage peptide libraries, displaying 7- or 12-residue peptides with random sequences fused to the N terminus of minor coat protein (pIII) (New England Biolabs, Ipswich, MA), were used according to manufacturer's recommendation for screening with mAb 5F1. Briefly, polystyrene plates coated with mAb 5F1 (10 μg/mL) and blocked with 0.2% casein were incubated with the phage peptide library ($\sim 10^{10}$ CFU). The supernatant was discarded, and plates were washed 10 times with TBS/Tween. Bound phages were eluted with 0.1 M glycine/HCl, pH 2.2, and the eluate was immediately neutralized with 1 M Tris-HCl, pH 8.0. The eluted phages were amplified by infecting *Escherichia coli* and used as input phages for the next round. Phage clones of the third and fourth round of biopanning were sequenced with the T7-sequence kit of Pharmacia. Alignment of the peptide sequences of the isolated clones with each other as well as with human ACE (full-length, two- domain ACE as well as individual N and C domains) was performed using the PIMA

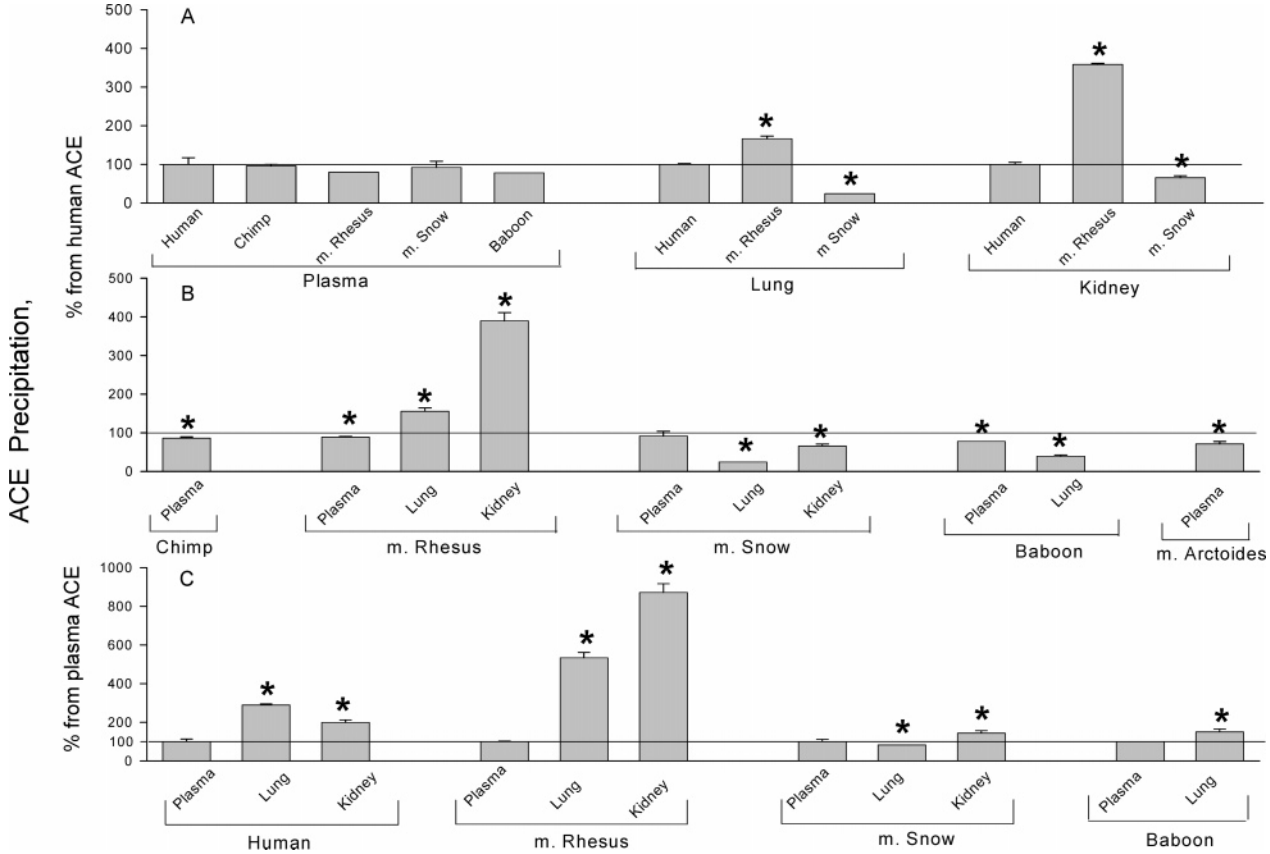

FIGURE 2: Cross-reactivity of mAb 5F1 with primate ACE. Plate precipitation assay. ACE activity in ACE from different tissues, lung, kidney, and plasma of different primate species, was adjusted to a final enzymatic activity of 5−10 milliunits/mL using Hip-His-Leu as a substrate. ACE preparations were then incubated with microtiter plates coated with mAb 5F1 as in Figure 1. Precipitated ACE activity was quantified spectrofluorometrically with Hip-His-Leu as a substrate (*17*). Data were presented as a percentage of precipitation of different ACEs to that of human ACE (panels A and B) and to that of plasma ACE (panel C).

multiple sequence alignment program (http://don.imgen.bcm.tmc.edu:9331/cgi-bin/multi-align/multi-align.pl).

Mutagenesis. The single N domain (D629) (*13*, *18*, *22*) was used as a starting point for mutagenesis studies. A series of six single amino acid substitutions in D629 cDNA were generated using a modification of the QuickChange site-directed mutagenesis protocol (Stratagene, La Jolla, CA), substituting the supplied polymerase with the high-fidelity *Pfu* polymerase (Promega Corp.). Complementary primers required for the introduction of point mutations were designed with WATCUT (Michael Palmer, University of Waterloo, Canada; http://watcut.uwaterloo.ca/watcut), using the restriction analysis and silent mutation analysis software, and purchased from Inqaba Biotechnical Industries (South Africa). Restriction enzyme sites were introduced through silent mutations to facilitate screening. Mutants were identified and confirmed by DNA sequence analysis. Mutated variants of the truncated N domain were transfected into CHO cells using the calcium phosphate method. These constructs do not contain a transmembrane anchor; therefore, the expressed ACE protein was secreted into the culture medium. Stable cell lines were grown in bulk, and serum-free culture medium (Gibco OPTIMEM, Invitrogen Corp.) was harvested from these transfected cells as a source of the mutated variants of the N-terminal domain of human ACE. These mutants are referred to by the single letter amino acid code for the wild-type protein and the position of this amino acid in the sequence, followed by the variant amino acid in single letter code, e.g., E49A.

Western Blotting. The purified N domain (D629), testis ACE (tACEΔ36), and chimeric mutants C1-141Ndom, C395-557Ndom, and C561-601Ndom were used for Western blotting, as well as supernatants of tissue homogenates from rat lung, rabbit lung, and mouse kidney. mAb 4G6, which recognizes both sACE and the isolated N domain, and polyclonal anti-tACE antibodies (generated against tACEΔ36) were used as positive controls. All samples for SDS−PAGE were equilibrated to a total ACE activity in 15−20 μL of 5 milliunits (Z-Phe-His-Leu) for detection by positive controls and 10 milliunits for mAb 5F1. Samples were resolved on 7% SDS−PAGE reducing gels and transferred by electrophoresis to nitrocellulose membrane (Hybond-ECL, Amersham Biosciences). Detection was carried out using the ECL-Plus horseradish peroxidase system (Amersham Biosciences).

Modeling of the N Domain Structure. A model of the N domain of human ACE in an open conformation was built previously (*18*), based on the unliganded structure of homologue ACE2 [PDB ID 1R42 (*31*)].

RESULTS

Previously, we demonstrated that one out of eight mAbs directed to the N domain of human ACE had an epitope that did not overlap with any of the others (*17*). This mAb was

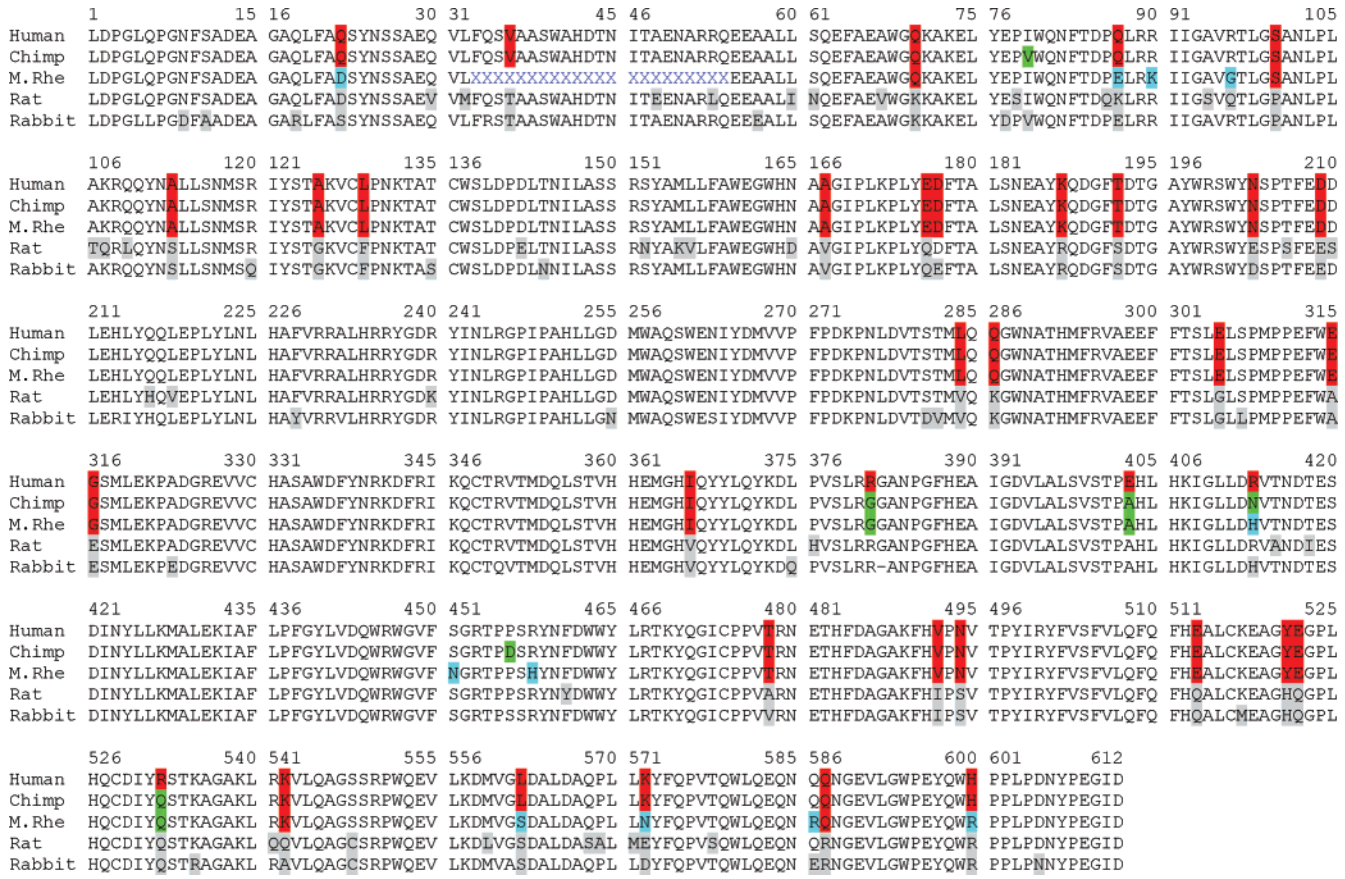

FIGURE 3: Alignment of the N domains of mammalian ACE. Amino acid residues unique for primate (human, chimpanzee, and Macaque) ACE are highlighted in red. Amino acid residues in chimpanzee ACE which differ from human ACE (but not from Macaque Rhesus ACE) are highlighted in green. Amino acid residues in Macaque ACE which differ from human ACE and chimpanzee ACE are highlighted in blue.

able to bind catalytically active ACE in solution as well as denatured ACE on a Western blot. Here we present a more detailed study of this antibody, mAb 5F1, and fine mapping of its epitope.

mAb 5F1 Binding to Different Types of Human ACE. Figure 1 demonstrates the relative binding of mAb 5F1 (and mAb 9B9 as a positive control) with ACE molecules of different origin and size: (1) recombinant human somatic ACE expressed in CHO cells in membrane-bound (1277 residues) and soluble (1203 residues) forms (*25*); (2) native somatic ACE from human lung and kidney (a mixture of membrane-bound and soluble ACE) and from plasma and ascitic and seminal fluids (soluble ACE); (3) truncated N fragments having 612 amino acid residues from the N domain and 17 amino acid residues from the interdomain linker, with (Nfr737) (*23*) and without (D629) (*16*, *18*, *22*) an additional 108 amino acid residues from the C domain; (4) a catalytically active ACE chimera C1-141Ndom (previously NdelACE) having the first 141 amino acid residues from the N domain and the rest from the C domain (*16*).

The relative precipitation of different ACEs varies significantly. mAb 5F1 binding to membrane-bound ACE (at least from lung and CHO cells) was significantly higher than to soluble ACE or truncated N fragments, while in contrast, binding of mAb 9B9 (positive control for precipitation of the N domain) to membrane-bound ACE is significantly lower than that of soluble ACE. The fact that precipitation of soluble ACE from seminal fluid by mAb 5F1 was significantly (2−3-fold) higher than precipitation of ACE by this mAb from plasma or ascitic fluid might be explained by the greater negative charge of blood ACE which carries more terminal sialic acid residues on its glycans. Interestingly, mAb 5F1 precipitated the ACE chimera C1-141Ndom where the first 141 amino acid residues from the N domain replaced the equivalent residues in the C domain. This indicates that one of the regions comprising the epitope for mAb 5F1 is present in the first 141 amino acid residues of the N domain. mAb 9B9 did not bind to this chimeric ACE at all.

mAb 5F1 Binding ACE from Different Species. In order to obtain further information about the localization of the epitope for mAb 5F1, we examined the cross-reactivity of mAb 5F1 with ACE from different species. Previously, we found that mAb 5F1 binds only to primate ACE (*17*, *32*). Figure 2 demonstrates the precipitation of ACE from different primate species by mAb 5F1. mAb 5F1 precipitation of plasma ACE from all primates studied [chimpanzee, Macaque Rhesus (*Macaca mulatta*), Japanese Snow Macaque (*Macaca fuscata*), Bear Macaque (*Macaca arctoides*), and baboon] was statistically lower than that of ACE from human plasma (Figure 2A,B). Lower precipitation relative to human ACE was also demonstrated for ACE from the lung and kidney of Macaque Snow and baboon. This indicates that the few substitutions in chimpanzee and Macaque Rhesus ACE (Figure 3) might be responsible for the observed decrease in mAb 5F1 binding to plasma ACE from these species. The amino acid sequence of the N domain of human ACE was aligned (Figure 3) with chimpanzee and Macaque

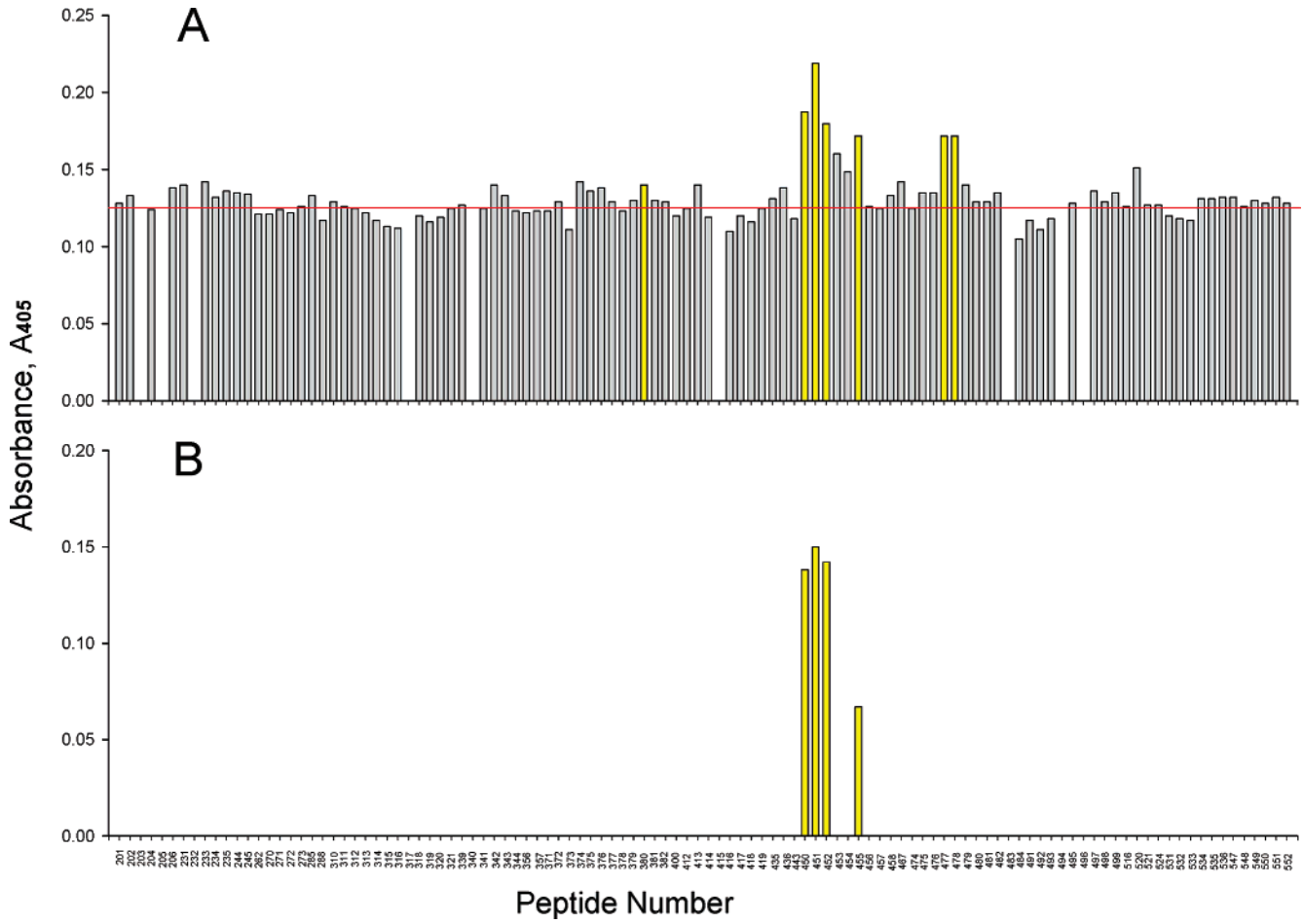

FIGURE 4: Binding of mAb 5F1 to synthetic peptides (ELISA). mAb 5F1 (10 μg/mL) was incubated with a set of 110 overlapping hexapeptides covering the human ACE sequence from residue 201 to residue 557 and immobilized on the pins in a 96-well format mictotiter plate (*30*). Mouse nonimmune IgG at the same concentration was used as a negative control. Bound mAb 5F1 was revealed using a second anti-mouse IgG conjugated with horseradish peroxidase. The *x*-axis shows peptide number, which is the sequence position of its first amino acid residue; the *y*-axis shows A_{450} values. Peptides showing significant binding to ACE are highlighted in yellow. (A) Representative experiment, with a red line indicating the cutoff for statistical significance with the mean of the lowest 50% of A_{450} values. (B) Statistical analysis of four independent experiments. Significant antibody binding to a hexapeptide was determined by an A_{405} value greater than the mean of the lowest 50% of all values, plus three times the standard deviation (*52*).

Rhesus ACE (which are recognized by mAb 5F1) and rat and rabbit ACE (which were not recognized by mAb 5F1). This alignment allowed the identification of primate-specific residues (colored red) as well as a few substitutions in chimpanzee and Macaque Rhesus ACE (colored green and blue, respectively; Figure 3).

Most of the substitutions in chimpanzee and Macaque Rhesus ACE may be excluded from being responsible for the decrease of mAb 5F1 binding relative to human ACE, on the basis that mAb 5F1 did not overlap with the other seven mAbs to the N domain (*17*), the epitopes of which were partially defined and found to be localized on one side of the N domain globule (*13*, *16*, *18*). Thus, of these substitutions, the most probable candidate for inclusion in the epitope of mAb 5F1 is the motif between S451 and R458 where three substitutions in chimpanzee and Macaque Rhesus ACE were found (Figure 3).

In contrast to plasma ACE, the precipitation of lung and kidney ACE from Macaque Rhesus was significantly higher than that from human, baboon, or Macaque Snow tissue (Figure 2B). This result might be indicative of a significantly different glycosylation pattern of ACE in Macaque Rhesus in comparison with human ACE and even more so in comparison with ACE from other primates (Figure 2C), which in turn might result in a lower proportion of sialic acid on those glycan moieties of Macaque Rhesus ACE which participate in the epitope for mAb 5F1.

Epitope Mapping with Synthetic Peptides Immobilized on Plastic Pins. In order to localize the epitope for mAb 5F1, a set of 110 overlapping hexapeptides covering the amino acid sequences of predicted epitopes on the N domain (residues 201−557, somatic ACE numbering) (*9*, *30*) were tested for 5F1 binding (Figure 4). In a representative experiment mAb 5F1 bound specifically with overlapping hexapeptides from two regions of the N domain starting from ^{450}F and ^{475}P (Figure 4A). Both of these regions have a double proline motif: ^{455}PP^{456} and ^{475}PP^{476}. mAb 5F1 reproducibly bound only to a motif from ^{450}F to ^{462}D (Figure 4B), with three standard deviations (SD) more mAb 5F1 binding to these pins than to the control.

Epitope Mapping with Phage Display Libraries. In order to confirm the epitope localization defined with the set of synthetic peptides, two phage libraries displaying peptides of different lengths (7- and 12-mer) were tested with mAb 5F1. After three rounds of selection with mAb 5F1 and amplification, 18 phage clones were isolated and sequenced.

Alignment

with full-size, two-domain ACE (1-277)			with truncated N domain (1-612)	
3_7	HDIY**PR**H			
7_12	RNHQT**HR**RQDGK			
7_7	T**HR**LLL			
5_12(2)	QPHTLSM**HR**HYY		T**PP**TSRAHAHYY	6_12(2)
3_12(2)	**S**PSDRLM**HNH**YH		**SPP**QSRA	6_7
5_7	MPH---I**HRH**		A**PP**XSPT	2_7
9_7	HPR**PR**NN		YPX**PP**LX	1_7
2_12	FAWXQ**HL**H**A**LEP		RQGGQY**P**	10_7
4_7	QG**HI**GNE		QRAT**PF**P	8_7
ACE	GLSQRLFSIRHRSL**HRH**SHG		**PP**SRYNFDWWYLRTKYQGIC**PP**VTRNNETH	ACE
	1246 1265		455 483	

FIGURE 5: Phage display peptide library screening with mAb 5F1. After three rounds of selection and amplification with mAb 5F1, 18 phage clones were isolated and sequenced. The phage sequences were aligned with each other and with the human somatic ACE sequence (1−1277) containing the highest degree of homology to the phage consensus motifs. Bold letters denote an exact match to the residues of human somatic ACE. The frequency of clones with the same sequences is denoted in parentheses. All sequences fall into two groups. Alignment of these sequences with each other and full-size ACE falls within amino acid residues 1256−1265 (in the cytoplasmic tail of ACE), whereas alignment with the N domain alone reveals similarity with amino acid residues 471−483.

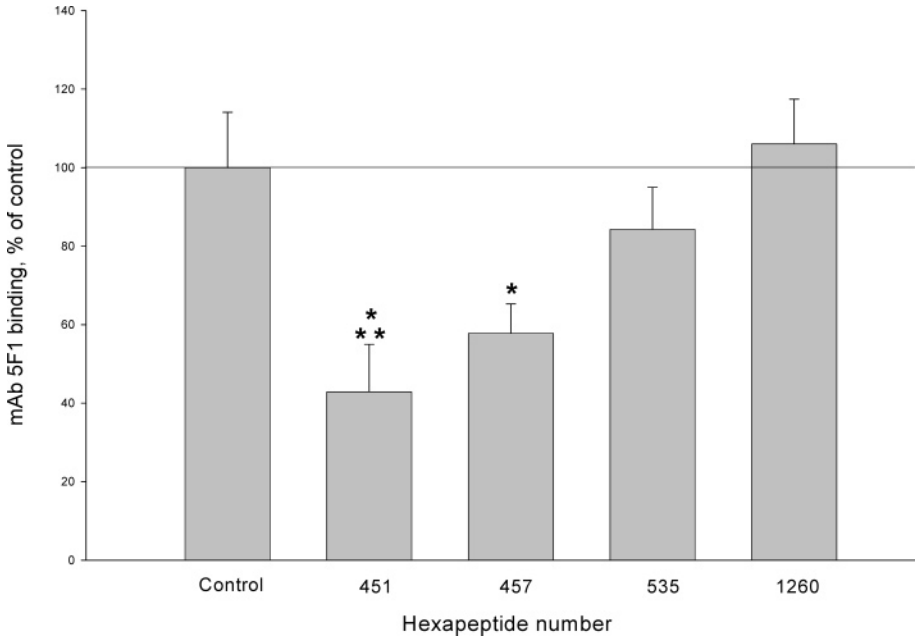

FIGURE 6: Competitive peptide ELISA. Microtiter wells were coated with purified human kidney ACE (5 μg/mL in 50 μL) and subsequently blocked with a solution of 0.2% casein. Peptide competitors were then added to some wells at concentrations of 0.25 and 1 mg/mL followed immediately by addition of anti-ACE mAb (10 μg/mL). The following hexapeptides, comprising a selection of sequences of ACE, were used: 451SGRTPP, 457SRYNFD, 535TKAGAL, and 1260RSLHRH. Bound mAb 5F1 was revealed with goat anti-mouse polyclonal antibody conjugated with alkaline phosphatase using *p*-nitrophenyl phosphate as a substrate and detected at 405 nm. Data are presented as a percentage of 5F1 binding (mean ± SD of two independent experiments in triplicate) in the presence of peptides relative to that in control wells without peptides.

Biopanning of the 7-mer library with mAb 5F1 resulted in the isolation of 10 independent phage clones, whereas biopanning of the 12-mer library revealed 8 independent phage clones. If the sequences of all 18 peptides are aligned with full-length human somatic ACE, the sequences align with the motif ^{1253}SIRHRSLHRHSHG^{1265}, with a consensus motif ^{1261}HRH^{1263}. However, if the alignment is performed with the N domain of ACE (amino acid residues from 1 to 612), the sequences align with the motif ^{474}CPPVTRNETH^{483}, with a consensus motif ^{475}PP^{476} (Figure 5). Moreover, individual alignment of the sequence of each phage with the ACE sequence did not reveal a consensus sequence, except for phages 2-7, 6-7, and 6-12, all of which were aligned with the motif ^{475}**PP**VT**R**N^{489}. On the basis of the hexapeptide binding evidence (Figure 4), however, we suggest that although PPVTRN was the only N domain sequence common to the tested phage peptides, this approach revealed a mimotope. Thus it would be misleading to conclude that ^{475}**PP**VT**R**N^{489} is part of the epitope for mAb 5F1; however, the detection of this sequence by phage display adds to the evidence that a double proline motif is included in the epitope.

Competitive Peptide ELISA. To confirm and further define the epitope for mAb 5F1, we performed a competitive peptide ELISA, where candidate peptides (synthesized in solution, not on pins) were tested for their ability to compete with mAb 5F1 for binding of human ACE immobilized on plastic. Both hexapeptides ^{451}SGRTPP and ^{457}SRYNFD competed with human kidney ACE immobilized on the plate for binding to mAb 5F1, whereas an unrelated peptide, ^{535}TKAGAL, and another candidate peptide, ^{1260}RSLHRH, did not compete with human ACE for mAb 5F1 binding (Figure 6). These results indicate that a motif between ^{451}S and ^{462}D is at least one of the regions included in the mAb

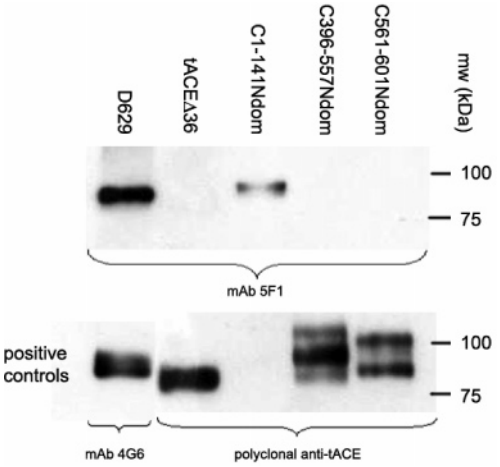

FIGURE 7: Western blot analysis of the binding specificity of mAb 5F1 to recombinant ACE fragments. The purified N domain (D629), testis ACE (tACEΔ36), and chimeric mutants C1-141Ndom (1−141), C396-557Ndom (396−557), and C561-601Ndom (561−601) were equilibrated to a total ACE activity in 15−20 μL of 5 milliunits (Z-Phe-His-Leu) for detection by positive controls and 10 milliunits for mAb 5F1. Samples were boiled and separated on 7% SDS−PAGE under reducing conditions. Proteins were transferred to nitrocellulose membranes and developed with mAb 5F1 (2 μg/mL) or with positive controls: antibody 4G6 (*34*), (positive control for the N domain), or polyclonal anti-tACE antibodies (tACEΔ36 and chimera are positive controls) in culture fluid. The molecular mass is shown on the right. After incubation with mAbs, binding was detected using the ECL-Plus horseradish peroxidase chemiluminescence system (Amersham Biosciences).

5F1 epitope, whereas the sequences around ^{475}PP and ^{1264}HRH probably represent mimotopes (*33*).

Western Blotting. In order to confirm the involvement of residues 1−141 in the 5F1 epitope as suggested by the earlier plate precipitation assays (Figure 1), we used Western blotting to investigate the binding of mAb 5F1 to three chimeric ACE mutants, comprising the C domain of ACE substituted with homologous regions of the N domain sequence. Equal amounts of active enzyme were blotted against mAb 5F1, with N domain-specific mAb 4G6 and polyclonal anti-tACE antibodies as positive controls.

Only C1-141Ndom, containing N domain residues 1−141, cross-reacted with mAb 5F1 (Figure 7). This supports the evidence from the plate precipitation assay regarding the importance of residues 1−141 and implies that N domain regions 395−557 and 561−601 alone are not sufficient for mAb 5F1 binding.

The fact that mAb 5F1 did not bind C396-557Ndom is surprising considering the evidence that residues around 451−462 are an important part of the epitope. However, it should be noted that this mAb was raised against the native N domain and that binding to the denatured N domain in Western blotting was weak in comparison with mAb 4G6, which was raised against the denatured N domain (*34*). Thus, it appears that the motif around 451−462 must be correctly folded in order for mAb 5F1 to bind and, therefore, that this motif is a structural, rather than a sequential, part of the epitope. The additional bands visible in the positive controls for C396-557Ndom and C561-601Ndom could be attributed to the presence of degradation products or improperly processed species in the purified samples, while the absence of a signal for C1-141Ndom in the positive controls probably indicates a higher activity of this mutant toward Z-Phe-His-Leu.

Residues 1−141 are not strongly conserved between primates and other mammals (Figure 3), which allowed us

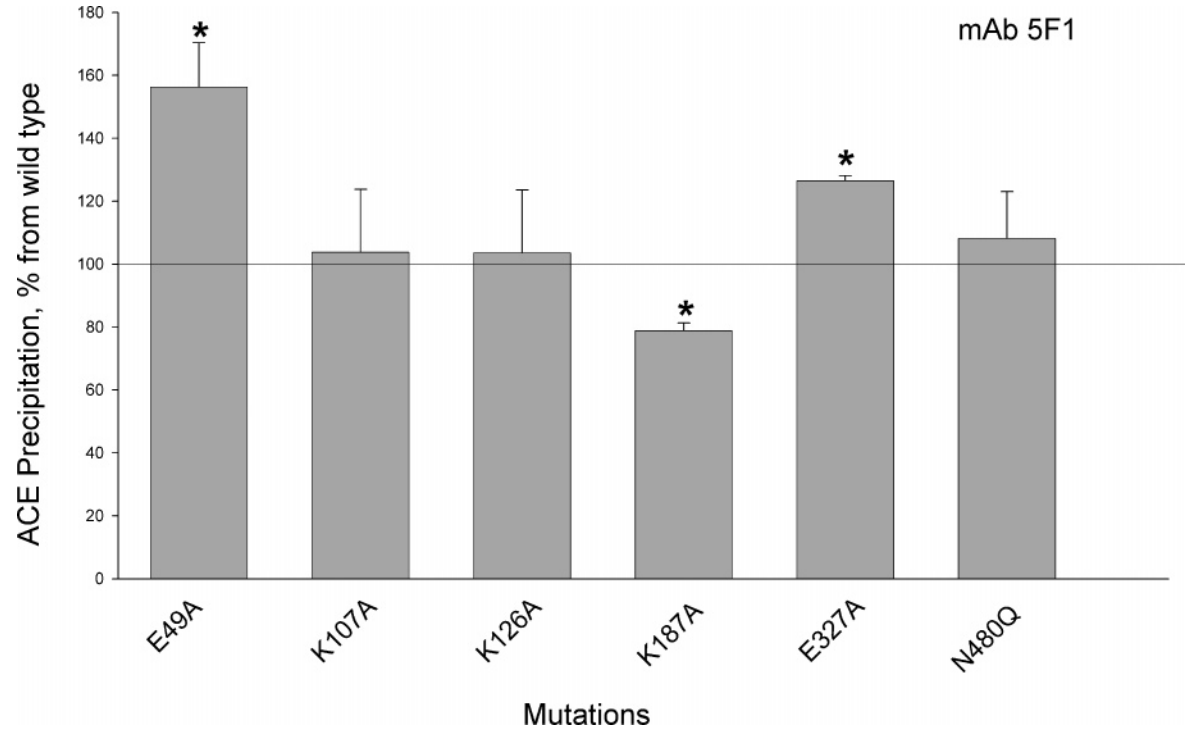

FIGURE 8: Effect of mutations on the precipitation of ACE activity by mAb 5F1. ACE activity of culture fluid from CHO cells expressing each mutant was equalized with ACE activity of the truncated N domain (D629), which was considered here as a wild-type ACE, in a range of 5−10 milliunits/mL (with Z-Phe-His-Leu as a substrate). Then precipitation of ACE activity of each mutant by mAb 5F1 was estimated by the plate precipitation assay. Results are expressed as a percentage of precipitated ACE activity from each mutant to that of the truncated N fragment and shown as the mean ± SD of four to six independent experiments, each in duplicates or triplicates.

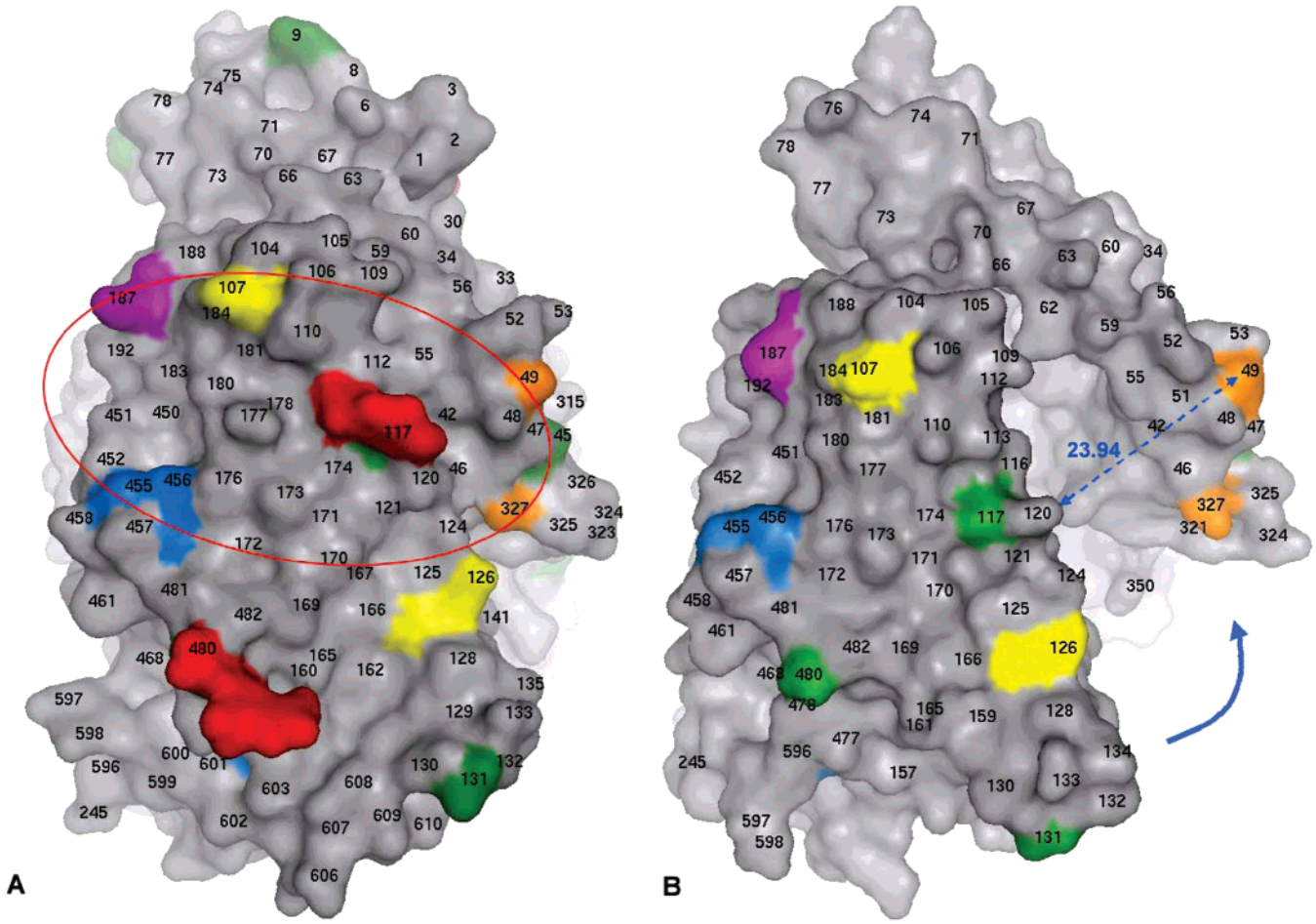

FIGURE 9: Fine epitope mapping for mAb 5F1. The epitope for mAb 5F1 was mapped onto the surface of (A) the substrate-bound crystal structure of the N domain of human ACE (PDB ID 2C6N) and (B) an open active site model of the N domain based on the unliganded structure of ACE2 (*18*). The surface is colored gray, with amino acid residues that were mutated to define the epitope for mAb 5F1 in colors as follows: residues whose substitution results in a significant increase in mAb 5F1 binding are colored orange; those causing a significant decrease are colored purple, and those having no effect are colored yellow (excluding glycosyation site N480, which is colored green). Note that the side chain of K187 is truncated in the crystal structure, probably due to its mobility. Asn residues at the N-linked glycosylation sites are colored green, while glycan residues observed in the crystal structure are colored red (*12*). Not all glycosylation sites had ordered glycan residues in the crystal structure, and no glycan residues were included in the modeled open form. Residues colored blue were suggested to be in the epitope for mAb 5F1 after screening the synthetic peptide libraries (Figure 4) and competition binding studies (Figure 5). The putative surface on ACE covered by mAb 5F1 is represented in (A) by an ellipse (red) with an approximate area of 880 Å^2, and an arrow in (B) indicates the lengthening of the epitope that would occur with opening of the active cleft.

to define the epitope for 5F1 in more detail. As mentioned above, we isolated 18 phage clones that bind to mAb 5F1 using the phage display technique (Figure 5). BLAST alignment of individual phage sequences with ACE revealed one phage from the 12-mer library (2-12) that aligned with ^{67}**AW**g**Q**kake**L**y**EP**^{78} and another from the 7-mer library (9-7) that aligned with ^{107}**KR**qqy**N**. Since the region around 107−112 is conserved in rabbit ACE but not in rat, the interaction of mAb 5F1 with ACE from these species allowed us to determine whether this motif is part of the epitope for 5F1. In a Western blotting experiment using tissue homogenates from these species, mAb 5F1 did not bind to rat or to rabbit ACE (data not shown), thus demonstrating that amino acids 106−109 are not an essential part of the mAb 5F1 epitope. The motif ^{67}**AW**g**Q**kake**L**y**EP**^{78} is mutated in both rat and rabbit ACE and thus could not be excluded by this experiment as a sequential part of the epitope for mAb 5F1.

Influence of Glycan Moieties on the Binding of mAb 5F1 to ACE. Altered glycosylation of human somatic ACE and the N domain by expression in CHO cells in the presence of NB-DNJ led to a significant increase in mAb 5F1 binding [201 ± 24% in comparison with untreated ACE ($p < 0.05$)]. In addition, we demonstrated that neuraminidase treatment of purified somatic ACE from seminal fluid led to increased precipitation of ACE activity by mAb 5F1 [123 ± 10% in comparison with untreated ACE ($p < 0.05$)]. Binding of mAb 5F1 also increased after treatment of human serum ACE with neuraminidase [179 ± 18% ($p < 0.05$)].

This indicates that (1) a glycan moiety is probably involved in the epitope for mAb 5F1 and (2) removal of sialic acid residues from glycan termini facilitates mAb 5F1 binding to somatic ACE. In contrast, enrichment of the sialic acid content as a result of ACE circulation in vivo (*35*) resulted in a dramatic (2−3-fold) decrease in mAb 5F1 binding to blood ACE (see Figure 1). Furthermore, the precipitation of ACE by mAb 5F1 depends to a great extent on the origin of the ACE sample. For example, precipitation of soluble human recombinant ACE expressed in COS and HEK cells was almost 3-fold higher (272 ± 23% and 285 ± 10%, $p < 0.05$, respectively), and precipitation of soluble ACE from human umbilical vein endothelial cells and macrophages was lower

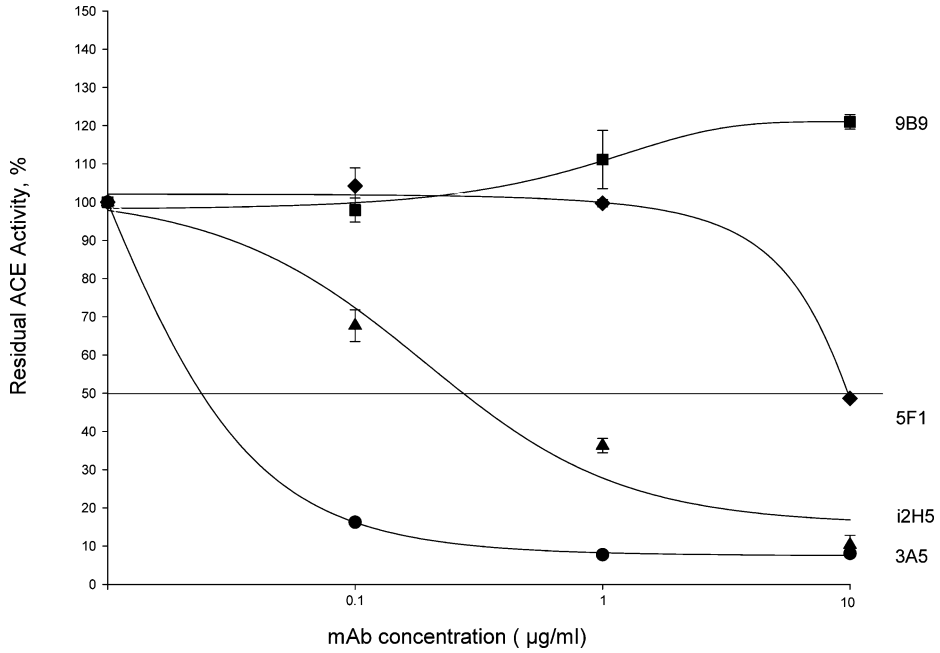

FIGURE 10: Anticatalytic effect of mAb 5F1 on the recombinant truncated N domain. Culture fluid from CHO cells transfected with the recombinant truncated N domain (D629) (10 milliunits/mL with Z-Phe-His-Leu as a substrate) was incubated with different mAbs to the N domain of ACE. Experimental conditions: [ACE] = 10 milliunits/mL; 100 mM potassium phosphate buffer containing 300 mM NaCl and 80 μM $ZnSO_4$, pH 8.3, at 37 °C. Results are shown as the mean ± SD of several (six to eight) experiments. mAb 9B9, which does not inhibit ACE catalytic activity (*17*), was used as a negative control, whereas mAbs 3A5 and i2H5, with strong anticatalytic potency (*18*), were used as positive controls. Residual ACE activity is expressed as the percentage of ACE activity remaining after mAbs were added to the reaction mixture.

(76 ± 12% and 72 ± 2%, $p < 0.05$) than that of ACE expressed in CHO cells. These data suggest that a glycan moiety is an integral part of the epitope for mAb 5F1.

Mutagenesis of the N Domain of ACE. In previous studies we defined the epitopes for some mAbs to the N domain of human ACE broadly by examining the cross-reactivity of these mAbs, raised against human ACE, with naturally occurring variants of ACE and described the differences in functional properties of these mAbs (*15*, *16*). However, the residues that could be evaluated were limited by the availability of amino acid sequences of naturally occurring variants. Replacement of specific amino acids in the N-terminal domain by site-directed mutagenesis allowed for a rational, systematic, and quantitative analysis of the interaction between antibodies and ACE.

Mutagenesis of amino acid residues for fine epitope mapping of mAb 5F1 was based on the following: (i) the epitope for 5F1 contains the motif ^{455}PP^{456} as well as residues which are specifically mutated in Macaque Rhesus; (ii) the surface area of the epitope should be between 500 and 900 Å^2 (*36*, *37*); (iii) the epitope for mAb 5F1 contains a glycosylation site.

Accordingly, a putative epitope was predicted on the basis of analysis of the N domain crystal structure (PDB ID 2C6N), and amino acids near the proposed epitope boundary were selected for mutation. Mutated residues are mostly protrusions on the protein surface, as these are more likely to form interactions with the antibody, and N480 is a glycosylation site. The selected residues were substituted with Ala or with Gln in the case of glycosylation site N480. Figure 8 demonstrates the effect of six mutations in the N-terminal domain on the binding of mAb 5F1. The effect of a mutation was considered to be of significance when a change in mAb binding of 10% or more was observed in comparison with the wild-type N domain (D629).

Of the six mutations, one (K187A) resulted in a significant decrease in mAb 5F1 binding, indicating that K187 forms an important part of the epitope, while three mutations (K107A, K126A, and N480Q) had no effect on mAb 5F1 binding, and two (E49A and E327A) caused an increase in binding (Figure 8). The increase in binding caused by E49A and E327A suggests that these amino acids may be included in the binding surface for mAb 5F1 and that their mutation to Ala facilitates a more favorable interaction. The negligible effect of the elimination of glycosylation site N480 suggests that a glycan at this site is not involved in mAb 5F1 binding. Similar substitutions of more than 25 amino acid residues in the N domain (*12*, *17*) did not change 5F1 binding.

Modeling of the N Domain of ACE and Fine Epitope Mapping. The determination of X-ray crystal structures of the C and N domains of human ACE (*10*, *11*), together with the site-directed mutagenesis data, made it possible to define the epitope for mAb 5F1 in fine detail (Figure 9). While the native N domain structure was reported to be nearly identical to the inhibitor-bound C domain structure (*11*), implying that no ligand-dependent conformational change occurs for the N domain, the presence of two ligands (acetate and *N*-carboxyalanine) bound to the active site of the enzyme suggests that this might represent another ligand-bound structure (*17*, *38*). For this reason we employed both the substrate-bound crystal structure of the N domain of ACE (PDB ID 2C6N) and an "open" conformation modeled on the structure of human ACE-related carboxypeptidase, ACE2 (PDB ID 1R42). Figure 9A shows the predicted epitope for mAb 5F1 on the surface of the N domain crystal structure. The epitope includes residues F450−D462 (identified using

PepScan and competitive peptide ELISA), E49, K187, and E327 (identified by mutagenesis), and glycosylation site N117. It excludes K126 and glycosylation site N480 (eliminated by mutagenesis) and is estimated to cover a surface area of approximately 700−900 Å^2. K107 is also included in the epitope; however, since mutation of this amino acid was shown to have a negligible effect on mAb 5F1 binding, this residue is probably not an essential part of the epitope. The majority of the amino acid residues in the epitope are charged or polar (65%), including one Arg, three Lys, four Glu, one His, and one Asp, while only 35% of the residues are hydrophobic, and most of these have their side chains buried in the core of the protein and their polar main-chain atoms exposed on the surface (Figure 9). The proximity of glycosylation site N45 to the epitope suggests that carbohydrate residues attached to this site might also participate in the epitope.

Inhibitory Activity of mAb 5F1. In the modeled open conformation of the N domain (Figure 9B), in which the active cleft opens by as much as 16 Å, E49 can be seen to move away from the remainder of the epitope. This apparently contradicts previous evidence that mAb 5F1 has no anticatalytic activity against ACE (*17*).

In order to investigate the inhibitory activity of mAb 5F1 further, the purified N domain (D629) was incubated with increasing concentrations of mAb 5F1 before determination of ACE activity with substrates Hip-His-Leu and Z-Phe-His-Leu. Figure 10 demonstrates that mAb 5F1 does inhibit ACE N domain activity at high concentrations (10 μg/mL, which represents an approximate 5-fold molar excess), while control mAb 9B9 has no inhibitory activity at this concentration. mAb 3A5 and i2H5 demonstrating a potent inhibitory activity (*18*) were used as a positive control for inhibition. The fact that no inhibition was detected at lower concentrations can be explained by the fact that mAb 5F1 binds more weakly to the N domain than the other mAbs tested and explains why inhibitory activity was not detected previously (*17*).

DISCUSSION

Monoclonal antibodies to ACE are extremely useful tools for the investigation of, among other things, enzyme functions and structural topography. In the case of human ACE, mAbs that recognize conformational epitopes on the N domain surface and sequential epitopes on the denatured C domain have been used successfully for the following: (i) ACE quantification both in solution by ELISA (*29*) and on the cell surface by flow cytometry (*6*), (ii) to study the structure and function of ACE (*13*−*19*), (iii) to deliver enzymes and genes to the pulmonary endothelium (*39*−*42*), (iv) as a diagnostic tool for lung vessel visualization (*43*, *44*), and (v) for immunohistochemistry (*22*, *45*−*49*).

In this study we performed fine epitope mapping of a monoclonal antibody to human ACE, 5F1, which is unique in that it binds catalytically active ACE in solution (*17*) and on the cell surface (*25*) as well as denatured ACE in Western blotting (*17*) and on paraffin-embedded sections (R. Metzger, unpublished observations). To this end a combination of screening of a synthetic peptide library based on the ACE sequence, random phage peptide library screening, Western blotting, and site-directed mutagenesis was used. The epitope was mapped onto the recently published structure of the N domain of human ACE (*12*), which represents the N domain in a so-called "closed conformation" (*11*, *18*) as well as an N domain model based on the 3D structure of ACE-related carboxypeptidase, ACE2 (*31*), which represents an "open conformation" of the N domain (Figure 9). Mapping of residues implicated in mAb 5F1 binding onto the surface of the molecule revealed that the epitope is large (approximately 700−900 Å^2) and confirmed its location to be quite far (more specifically, on the other side of the N domain globule) from the epitopes for the other seven mAbs to the N domain of ACE which we developed (*16*−*19*).

Synthetic peptide library screening allowed us to identify at least one part of the epitope for mAb 5F1, residues ^{454}-TPPSRYN^{460}, which was also suggested by comparison of the sequences of ACE from various primates (Figures 3, 4, and 6). It is worth noting that this motif is part of one of the immunodominant regions on the N domain, which were revealed recently using polyclonal antibodies to ACE and PepScan technology (*30*). However, we did not isolate the same, or any other mAb 5F1-related, sequence using a phage peptide library (Figure 5). The observed low similarity between the selected phage inserts and the sequence of ACE is most likely due to the fact that the sequence of interest is not guaranteed to be present in a commercially available phage library such as that employed here. This fact has been noted to have important implications especially for longer epitopes since these are less likely to be present in their entirety (*50*). Furthermore, the techniques of peptide scanning and phage display are limited in their ability to characterize epitopes that are conformational in nature rather than only sequence-dependent, as seems to be the case for mAb 5F1. In the absence of a complete complementary phage sequence, mimotopes may be identified that take on a similar conformation to the epitope while appearing to be unrelated in sequence (*33*), as was seen in this case with a double proline motif (Figure 5). The failure to isolate a true antigen-homologous peptide and instead to identify only mimotope sequences is not uncommon (*51*). The conformation-dependent, as opposed to sequence-driven, nature of 5F1 binding to this part of the epitope is supported by the fact that mAb 5F1 did not bind a denatured ACE chimera containing both double proline motifs identified by peptide library scanning (Figure 7).

A sequential element of the mAb 5F1 epitope is present in the first 141 residues of the N domain, as evidenced by the detection of a denatured chimera containing this sequence, by Western blotting (Figure 7). On the basis of our fine mapping (Figure 9), this sequence is likely to include residues around N117 or K126. Residues 106−109 were excluded as candidates on the basis of the lack of mAb 5F1 binding to rabbit ACE (data not shown), which has this sequence intact.

In agreement with the observed effect of different glycosylation states on substrate binding, the mAb 5F1 epitope includes a glycosylation site, N117. This strong glycosylation dependence implies that the glycan moiety attached to N117 is quite different in different tissues and cells and suggests that binding of mAb 5F1 might be used as a tool for discriminating between ACE from different sources. It should be noted that only single glycan residues from two glycosylation sites near the epitope were present in the crystal structure but that in vivo these glycan chains might be many residues long, containing branch sites and charged sialic

acids. Thus the increase in binding following deglycosylation or desialation probably results from a removal of glycan residues that otherwise partially obscure the binding site for mAb 5F1. It is interesting that despite its proximity to the epitope, elimination of the glycan at N480 by mutation did not alter mAb 5F1 binding significantly. However, a third glycosylation site, N45, which was not mutated, is close to the edge of the epitope, so that an extended glycan chain at this site might also participate in mAb 5F1 binding.

Mutagenesis experiments aimed at delineating the boundaries of the epitope revealed the importance of two residues, E49 and E327 (Figure 8), that lie on the opposite side of the active cleft from the rest of the epitope, as predicted by the open model of the N domain (Figure 9B). During the opening of the active cleft depicted by this model, E49 and E327 move away from the remainder of the epitope by approximately 20 Å, a movement too large to be encompassed by the surface of association with mAb 5F1 since this area also includes K187 and must be smaller than 900 Å^2. Logically then, these residues could not all be included in an epitope for mAb 5F1 that also allowed the active cleft to open and the substrate to bind while the antibody was in place. This finding was surprising to us, as a previous study had not attributed any inhibitory activity of ACE to mAb 5F1(*17*). However, when increasing concentrations of mAb 5F1 were added to the ACE N domain before assaying for ACE activity, inhibition was observed at 10 μg/mL mAb 5F1, a concentration higher than had previously been used to assess inhibition (*17*). This result not only validates our mapping of the epitope of mAb 5F1 but also confirms the predicted importance of the opening of the active site cleft in order to allow substrate binding in ACE (*18*, *38*). Moreover, it seems to implicate a small number of residues (those around E49) in this process, consistent with a hinge-bending motion such as that seen in ACE2, excluding any other candidate openings which are not in the vicinity of the epitope. However, we cannot entirely exclude the possibility that mAb 5F1 binding stabilizes the interactions between secondary structure elements which must move in order to allow opening at a distant site, as has been observed previously (*18*).

Thus we have made use of a combination of different methods to define the epitope for mAb 5F1, an antibody that recognizes both catalytically active and denatured ACE, and by means of this process have identified a possible use for mAb 5F1 in studying ACE glycoforms and uncovered further evidence for the importance of hinge bending in the catalytic activity of ACE.

ACKNOWLEDGMENT

We are grateful to Dr. V. Gavrilyuk (then at the University of Illinois at Chicago) for help with analysis of the synthetic peptide and phage display peptide library screening. We thank Sylva Schwager, Pierre Redelinghuys, and Wendy Kröger for assisting with the preparation of ACE constructs.

REFERENCES

1. Ehlers, M. R. W., and Riordan, J. F. (1989) Angiotensin-converting enzyme: new concepts concerning its biological role, *Biochemistry 28*, 5311−5318.
2. Skidgel, R. A., and Erdos, E. G. (1993) Biochemistry of angiotensin I-converting enzyme, in *The Renin-Angiotensin System* (Robertson, J. I. S., and Nichols, M. G., Eds.) pp 10.1−10.10, Glower Medical Publishing, New York.
3. Corvol, P., Eyries, M., and Soubrier, F. (2004) Peptidyl-dipeptidase A/Angiotensin I-converting enzyme, in *Handbook of Proteolytic Enzymes* (Barret, A. A., Rawlings, N. D., and Woessner, J. F., Eds.) pp 332−349, Elsevier Academic Press, New York.
4. Dzau, V. J., Bernstein, K., Celermajer, D., Cohen, J., Dahlof, B., Deanfield, J., Diez, J., Drexler, H., Ferrari, R., van Gilst, W., Hansson, L., Hornig, B., Husain, A., Johnston, C., Lazar, H., Lonn, E., Luscher, T., Mancini, J., Mimran, A., Pepine, C., Rabelink, T., Remme, W., Ruilope, L., Ruzicka, M., Schunkert, H., Swedberg, K., Unger, T., Vaughan, D., and Weber, M. (2001) The relevance of tissue angiotensin-converting enzyme: manifestations in mechanistic and endpoint data, *Am. J. Cardiol. 88* (Suppl.), 1L−20L.
5. Balyasnikova, I. V., Danilov, S. M., Muzykantov, V. R., and Fisher, A. B. (1998) Modulation of angiotensin-converting enzyme in cultured human vascular endothelial cells, *In Vitro Dev. Biol. Anim. 34*, 545−554.
6. Danilov, S. M., Sadovnikova, E., Scharenborg, N., Balyasnikova, I. V., Svinareva, D. A., Semikina, E. L., Parovichnikova, E. N., Savchenko, V. G., and Adema, G. J. (2003) Angiotensin-converting enzyme (CD143) is abundantly expressed by dendritic cells and discriminates human monocyte-derived dendritic cells from acute myeloid leukemia-derived dendritic cells, *Exp. Hematol. 31*, 1301−1309.
7. Danilov, S. M., Franke, F. E., and Erdos, E. G. (1997) Angiotensin-converting enzyme (CD143), in *Leucocyte Typing VI: White cell differentiation antigens* (Kishimoto, T., et al., Eds.) pp 746−749, Garland Publishing, New York.
8. Franke, F. E., Metzger, R., Bohle, R.-M., Kerkman, L., Alhenc-Gelas, F., and Danilov, S. M. (1997) Angiotensin I-converting enzyme (CD 143) on endothelial cells in normal and in pathological conditions, in *Leucocyte Typing VI: White cell differentiation antigens* (Kishimoto, T., et al., Eds.) pp 749−751, Garland Publishing, New York.
9. Soubrier, F., Alhenc-Gelas, F., Hubert, C., Allegrini, J., John, M., Tregear, G., and Corvol, P. (1988) Two putative active centers in human angiotensin I-converting enzyme revealed by molecular cloning, *Proc. Natl. Acad. Sci. U.S.A. 85*, 9386−9390.
10. Ehlers, M. R., Fox, E. A., Strydom, D. J., and Riordan, J. F. (1989) Molecular cloning of human testicular angiotensin-converting enzyme: the testis isozyme is identical to the C-terminal half of endothelial angiotensin-converting enzyme, *Proc. Natl. Acad. Sci. U.S.A. 86*, 7741−7745.
11. Natesh, R., Schwager, S. L., Sturrock, E. D., and Acharya, K. R. (2003) Crystal structure of the human angiotensin-converting enzyme-lisinopril complex, *Nature 421*, 551−554.
12. Corradi, H. R., Schwager, S. L., Nchinda, A. T., Sturrock, E. D., and Acharya, K. R. (2006) Crystal structure of the N domain of human somatic angiotensin I-converting enzyme provides a structural basis for domain-specific inhibitor design, *J. Mol. Biol. 357*, 964−974.
13. Balyasnikova, I. V., Skirgello, O. E., Binevski, P. V., Nesterovitch, A. B., Albrecht, R. F., II, Kost, O. A., and Danilov, S. M. (2007) Monoclonal antibodies 1G12 and 6A12 to the N domain of human angiotensin-converting enzyme:fine epitope mapping and antibody-based method for revelation and quantification of ACE inhibitors in the human blood, *J. Proteome Res.* (in press.)
14. Balyasnikova, I. V., Karran, E. H., Albrecht, R. F., II, and Danilov, S. M. (2002) Epitope-specific antibody-induced cleavage of angiotensin-converting enzyme from the cell surface, *Biochem. J. 362*, 585−595.
15. Kost, O. A., Balyasnikova, I. V., Chemodanova, E. E., Nikolskaya, I. I., Albrecht, R. F., II, and Danilov, S. M. (2003) Epitope-dependent blocking of the angiotensin-converting enzyme dimerization by monoclonal antibodies to N-terminal domain of ACE: Possible Link of ACE dimerization and shedding from the cell surface, *Biochemistry 42*, 6965−6976.
16. Balyasnikova, I. V., Woodman, Z. L., Albrecht, R. F., II, Natesh, R., Acharya, K. R., Sturrock, E. D., and Danilov, S. M. (2005) Localization of an N domain region of angiotensin-converting enzyme involved in the regulation of ectodomain shedding using monoclonal antibodies, *J. Proteome Res. 4*, 258−267.
17. Danilov, S., Jaspard, E., Churakova, T., Towbin, H., Savoie, F., Lei, W., and Alhenc-Gelas, F. (1994) Structure-function analysis of angiotensin I-converting enzyme using monoclonal antibodies, *J. Biol. Chem. 269*, 26806−26814.

18. Skirgello, O. E., Balyasnikova, I. V., Binevski, P. V., Sun, Z.-L., Baskin, I. I., Palyulin, V. A., Nesterovitch, A. B., Albrecht, R. F., II, Kost, O. A., and Danilov, S. M. (2006) Inhibitory antibodies to human angiotensin-converting enzyme: fine epitope mapping and mechanism of action, *Biochemistry 45*, 4831−4847.
19. Danilov, S. M., Deinum, J., Balyasnikova, I. V., Sun, Z. L., Kramers, C., Hollak, C. E., and Albrecht, R. F. (2005) Detection of mutated angiotensin I-converting enzyme by serum/plasma analysis using a pair of monoclonal antibodies, *Clin. Chem. 51*, 1040−1043.
20. Stanislav, M. L., Balabanova, R. M., Alekperov, R. T., Miagkova, M. A., Abramenko, T. V., Kiselev, I. P., Kost, O. A., Nikolskaya, I. I., and Garats, E. V. (2001) Autoantibodies to vasoactive peptides and angiotensin converting enzyme in patients with systemic diseases of the connective tissue, *Ter. Arkh. 73*, 20−25.
21. Yu, X. C., Sturrock, E. D., Wu, Z., Biemann, K., Ehlers, M. R., and Riordan, J. F. (1997) Identification of N-linked glycosylation sites in human testis angiotensin-converting enzyme and expression of an active deglycosylated form, *J. Biol. Chem. 272*, 3511−3519.
22. Balyasnikova, I. V., Metzger, R., Franke, F. E., and Danilov, S. M. (2003) Monoclonal antibodies to denatured human ACE (CD143): broad species specificity, reactivity on paraffin-section, and detection of subtle conformational changes in the C-terminal domain of ACE, *Tissue Antigens 61*, 49−62.
23. Wei, L., Alhenc-Gelas, F., Corvol, P., and Clauser, E. (1991) The two homologous domains of human angiotensin I-converting enzyme are both catalytically active, *J. Biol. Chem. 266*, 9002−9008.
24. Woodman, Z. L., Schwager, S. L., Redelinghuys, P., Chubb, A. J., van der Merwe, E. L., Ehlers, M. R., and Sturrock, E. D. (2006) Homologous substitution of ACE C domain regions with N domain sequences: effect on processing, shedding, and catalytic properties, *Biol. Chem. 387*, 1043−1051.
25. Balyasnikova, I. V., Gavriljuk, V. D., McDonald, T. D., Berkowitz, R., Miletich, D. J., and Danilov, S. M. (1999) Antibody-mediated lung endothelium targeting: *In vitro* model using a cell line expressing angiotensin-converting enzyme, *Tumor Targeting 4*, 70−83.
26. Ehlers, M. R., Chen, Y. N., and Riordan, J. F. (1991) Purification and characterization of recombinant human testis angiotensin-converting enzyme expressed in Chinese hamster ovary cells, *Protein Expression Purif. 2*, 1−9.
27. Pilliquod, Y., Reinharz, A., and Roth, M. (1970) Studies on the angiotensin-converting enzyme with different substrates, *Biochim. Biophys. Acta 206*, 136−142.
28. Friedland, J., and Silverstein, E. (1976) A sensitive fluorometric assay for serum angiotensin-converting enzyme, *Am. J. Clin. Pathol. 66*, 416−424.
29. Danilov, S. M., Savoie, F., Lenoir, B., Jeunemaitre, X., Azizi, M., Tarnow, L., and Alhenc-Gelas, F. (1996) Development of enzyme-linked immunoassays for human angiotensin I converting enzyme suitable for large-scale studies, *J. Hypertens. 14*, 719−727.
30. Kugaevskaya, E. V., Kolesanova, E. F., Kozin, S. A., Veselovskay, A. V., Dedinsky, I. R., and Elisseeva, Y. E. (2006) Epitope mapping of the domains of human angiotensin converting enzyme, *Biochim. Biophys. Acta 1760*, 959−965.
31. Towler, P., Staker, B., Prasad, S. G., Menon, S., Tang, J., Parsons, Th., Ryan, D., Fisher, M., Williams, D., Dales, N. A., Patane, M. A., and Pantoliano, M. W. (2004) ACE2 X-ray structures reveal a large hinge-bending motion important for inhibitor binding and catalysis, *J. Biol. Chem. 279*, 17996−18007.
32. Balyasnikova, I. V., Yeomans, D. C., McDonald, T. B., and Danilov, S. M. (2002) Antibody-mediated lung endothelium targeting: *in vivo* model on primates, *Gene Ther. 9*, 282−290.
33. Geysen, H. M., Rodda, S. G., and Mason, T. J. (1986) *A priori* delineation of a peptide which mimics a discontinuous antigenic determinant, *Mol. Immunol. 23*, 709−715.
34. Balyasnikova, I. V., Metzger, R., Sun, Z.-L., Berestetskaya, Y. V., Albrecht, R. A., II, and Danilov, S. M. (2005) Development and characterization of rat monoclonal antibodies to denatured mouse angiotensin-converting enzyme, *Tissue Antigens 65*, 240−251.
35. Lanzillo, J. J., Stevens, J., Tumas, J., and Fanburg, B. L. (1983) Spontaneous change of human plasma angiotensin I converting enzyme isoelectric point, *Arch. Biochem. Biophys. 227*, 434−439.
36. Mylvaganam, S. E., Paterson, Y., and Gertzoff, E. D. (1998) Structural basis for the binding of an anti-cytochrome antibody to its antigen: crystal structures of Fab E8-cytochrome *c* complex to 1.8Å resolution and FabE8 to 2.26Å resolution, *J. Mol. Biol. 281*, 301−322.
37. Huang, M., Syed, R., Stura, E. A., Sone, M. J., Stefanko, R. S., Ruf, W., Edgington, T. S., and Wilson, I. A. (1998) The mechanism of an inhibitory antibody on TF-initiated blood coagulation revealed by the crystal structures of human tissue factor, Fab 5G9 and TF-5G9 complex, *J. Mol. Biol. 275*, 873−894.
38. Watermeyer, J. M., Sewell, B. T., Schwager, S. L., Natesh, R., Corradi, H. R., Acharya, K. R., and Sturrock, E. D. (2006) Structure of testis ACE glycosylation mutants and evidence for conserved domain movement, *Biochemistry 45*, 12654−12663.
39. Muzykantov, V. R., Atochina, E. N., Ischiropoulos, H., Danilov, S. M., and Fisher, A. B. (1996) Immunotargeting of antioxidant enzymes to the pulmonary endothelium, *Proc. Natl. Acad. Sci. U.S.A. 93*, 5213−5218.
40. Atochina, E. N., Balyasnikova, I. V., Danilov, S. M., Granger, D. N., Fisher, A. B., and Muzykantov, V. R. (1998) Catalase targeting to the surface endothelial antigens protects pulmonary vasculature against oxidative insult, *Am. J. Physiol. 275*, L806−L817.
41. Reynolds, P. N., Zinn, K. R., Gavrilyuk, V. D., Balyasnikova, I. V., Rogers, B. E., Buchsbaum, D. J., Wang, M. H., Miletich, D. J., Crizzle, W. E., Douglas, J. T., Danilov, S. M., and Curiel, D. T. (2000) A targetable, injectable adenoviral vector for selective gene delivery to pulmonary endothelium, *in vivo*, *Mol. Ther. 2*, 562−578.
42. Muller, W. H., Brosnan, M. J., Graham, D., Nicol, C. G., Morecroft, I., Channon, K. M., Danilov, S. M., Reynolds, P. N., Baker, A. H., and Dominiczak, A. F. (2005) Targeting endothelial cells with adenovirus expressing nitric oxide synthase prevents elevation of blood pressure in stroke-prone spontaneously hypertensive rats, *Mol. Ther. 12*, 321−327.
43. Danilov, S. M., Martynov, A., Klibanov, A. L., Slinkin, M. A., Sakharov, I. Y., Malov, A. G., Sergienko, V. B., Vedernikov, A. Y., Muzykantov, V. R., and Torchilin, V. P. (1989) Radioimmunoimaging of lung vessels: an approach using 111-In-labeled monoclonal antibody to angiotensin-converting enzyme, *J. Nucl. Med. 30*, 1688−1692.
44. Muzykantov, V. R., and Danilov, S. M. (1995) Targeting of radiolabelled monoclonal antibody against angiotensin-converting enzyme to the pulmonary vasculature, in *Handbook of Targeting Delivery of Imaging Agents* (Torchilin, V. P., Ed.) pp 465−486, CRC Press, Boca Raton, FL.
45. Danilov, S. M., Faerman, A. I., Printseva, O. Y., Martynov, A. V., Sakharov, I. Y., and Trakht, I. N. (1987) Immunohistochemical study of angiotensin-converting enzyme in human tissues using monoclonal antibodies, *Histochemistry 87*, 487−490.
46. Metzger, R., Bohle, R.-M., Kerkman, L., Eichner, G., Alhenc-Gelas, F., Danilov, S. M., and Franke, F. E. (1999) Distribution of angiotensin I-converting enzyme (CD 143) in the normal human kidney and in non-neoplastic kidney diseases, *Kidney Int. 56*, 1442−1454.
47. Metzger, R., Bohle, R.-M., Chumachenko, P., Danilov, S. M., and Franke, F. E. (2000) CD 143 in the development of atherosclerosis, *Atherosclerosis 150*, 21−31.
48. Franke, F. E., Fink, L., Kerkman, L., Steger, K., Klonisch, T., Metzger, R., Alhenc-Gelas, F., Burkhard, E., Bergmann, M., and Danilov, S. M. (2000) Somatic isoform of angiotensin-converting enzyme in the pathology of testicular germ cell tumors, *Human Pathol. 31*, 1466−1476.
49. Pauls, K., Metzger, R., Steger, K., Klonisch, T., Danilov, S., and Franke, F. E. (2003) Isoforms of angiotensin I-converting enzyme in the development and differentiation of human testis and epididymis, *Andrologia 35*, 32−43.
50. Bottger, V., Stasiak, P. C., Harrison, D. L., Mellerick, D. M., and Lane, E. B. (1995) Epitope mapping of monoclonal antibodies to keratin 19 using keratin fragments, synthetic peptides and phage peptide libraries, *Eur. J. Biochem. 231*, 475−485.
51. Kola, A., Baensch, M., Bautsch, W., Hennecke, M., Klos, A., Casareto, M., and Kohl, J. (1996). Epitope mapping of a C5a neutralizing mAb using a combined approach of phage display, synthetic peptide and site directed mutagenesis, *Immunotechnology 2*, 115−126.
52. Worthington, J., and Morgan, K. (1994) Epitope mapping using synthetic peptides, in *Peptide Antigens. A practical approach* (Wisdom, G. B., Ed.) pp 181−217, Oxford University Press, Oxford.

BI700489V